Cloud-Drift and Water Vapor Winds in the Polar Regions From MODIS

Jeffrey R. Key, David Santek, Christopher S. Velden, Niels Bormann, Jean-Noël Thépaut, Lars Peter Riishojgaard, Yanqiu Zhu, and W. Paul Menzel

***Abstract*—Wind products from geostationary satellites have been generated for over 20 years and are now used in numerical weather prediction systems. However, geostationary satellites are of limited utility poleward of the midlatitudes. This study demonstrates the feasibility of deriving high latitude tropospheric wind information from polar-orbiting satellites. The methodology employed is based on the algorithms currently used with geostationary satellites, modified for use with the Moderate-Resolution Imaging Spectroradiometer (MODIS) infrared window and water vapor bands. These bands provide wind information throughout the troposphere in both clear and cloudy conditions. The project presents some unique challenges, including the irregularity of temporal sampling, varying viewing geometries, and uncertainties in wind vector height assignment as a result of low atmospheric water vapor amounts and thin clouds. A 30-day case study dataset has been produced and is being used in model impact studies. Preliminary results are encouraging: when the MODIS winds are assimilated in the European Centre for Medium Range Weather Forecasts (ECMWF) system and the NASA Data Assimilation Office system, forecasts of the geopotential height for the Arctic, the Northern Hemisphere extratropics, and the Antarctic are improved significantly.**

***Index Terms*—MODIS, numerical weather prediction, polar meteorology, satellite applications, winds.**

I. Introduction

IN THE EARLY 1960s, Tetsuya Fujita developed analysis techniques to use cloud pictures from the first TIROS polar orbiting satellite for estimating the velocity of tropospheric winds [14]. Throughout the 1970s and early 1980s, cloud motion winds were produced from geostationary satellite data using a combination of automated and manual techniques. In 1992, the National Oceanic and Atmospheric Administration (NOAA) began using an experimental automated winds software package developed at the University of Wisconsin Space Science and Engineering Center that made it possible to produce a full-disk wind set without manual intervention. The carbon dioxide (CO_2) slicing algorithm [15] made it possible to assign more accurate cloud heights to the motion vectors. Cloud-drift winds were used in numerical weather prediction systems as early as the 1980s. Fully automated cloud-drift and water vapor motion vector production from the Geostationary Operational Environmental Satellites (GOES) became operational in 1996, and now wind vectors are routinely used in operational numerical models of the National Centers for Environmental Prediction (NCEP) [17].

Satellite-derived wind fields are most valuable where few observations exist and model analyses are less accurate as a result. Like the oceans at lower latitudes, the polar regions suffer from a lack of observational data. Fig. 1 illustrates the sparse observation network in the Arctic and Antarctic. World Meteorological Organization (WMO) stations, which provide regular wind observations from rawinsondes, are scattered across the coastal areas and the interior of Canada, Alaska, Russia, and northern Europe. However, there is little or no coverage of the interior of Greenland, the interior of Antarctica, the Arctic Ocean, and the oceans surrounding Antarctica.

A recent study by [5] gives evidence that the existing observation network is not sufficient for accurate predictions of high-latitude wind fields. The study examined tropospheric winds in the National Centers for Environmental Prediction/National Center for Atmospheric Research (NCEP/NCAR) Reanalysis and the European Centre for Medium Range Weather Forecasts (ECMWF) Reanalysis datasets. Rawinsonde data from two Arctic field experiments (CEAREX in 1988 and LeadEx in 1992) that were not assimilated by the models were used as independent validation and compared to reanalysis products for five tropospheric vertical layers. It was found that both reanalyses exhibit large biases in zonal and meridional wind components, being too westerly and too northerly. It was also found that reanalysis winds were too strong by 25% to 65% relative to the rawinsonde values.

Unfortunately, geostationary satellites are of little use at high latitudes due to poor viewing geometry, resulting in large uncertainties in the derived wind vectors. Can polar-orbiting satellites be used to obtain wind information at high latitudes? The idea has been previously explored with some promising results. The Advanced Very High Resolution Radiometer (AVHRR) was used by Herman [7] to estimate cloud-drift winds for a few Arctic scenes. When compared to rawinsonde winds, the AVHRR winds were found to have an rms difference of 6 m/s. Herman and Nagle [8] compared cloud-drift winds from the AVHRR to gradient winds computed with the High-Resolution Infrared Sounder (HIRS). The AVHRR winds were found to be comparable to the HIRS gradient winds,

Manuscript received April 29, 2002; revised October 14, 2002. This work was supported by an NOAA Grant NA07EC0676 and NASA Grant NAS5-31367.

J. R. Key and W. P. Menzel are with the Office of Research and Applications, National Oceanic and Atmospheric Administration, National Environmental Satellite, Data, and Information Service, Madison, WI 53706 USA (e-mail: jkey@ssec.wisc.edu).

D. Santek and C. S. Velden are with the Cooperative Institute for Meteorological Satellite Studies, University of Wisconsin, Madison, WI 53706 USA.

N. Bormann and J.-N. Thépaut are with the European Centre for Medium Range Weather Forecasts, Shinfield Park, Reading, Berkshire, RG2 9AX U.K.

L. P. Riishojgaard and Y. Zhu are with the Data Assimilation Office, NASA Goddard Space Flight Center, Greenbelt, MD 20771 USA.

Digital Object Identifier 10.1109/TGRS.2002.808238

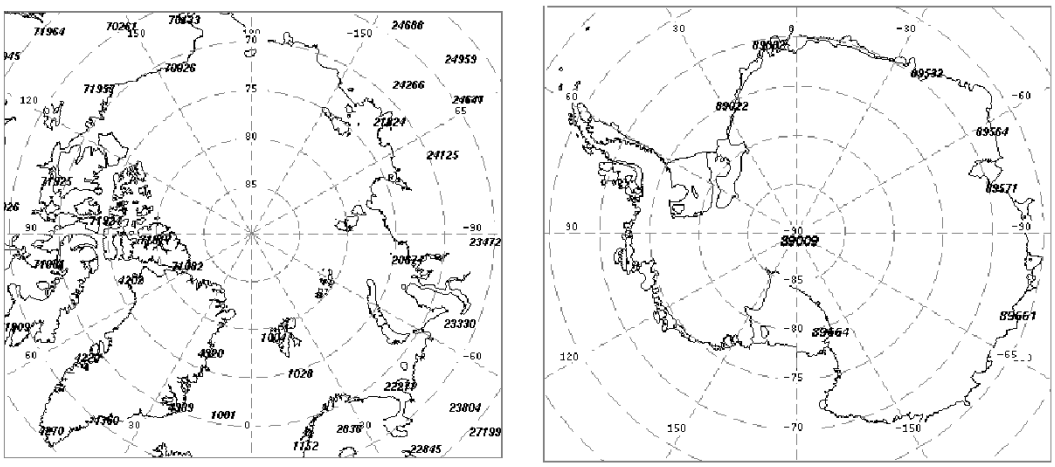

(a) (b)

Fig. 1. WMO stations across (a) the Arctic and (b) the Antarctic. Only those stations that provide regular daily wind data are shown.

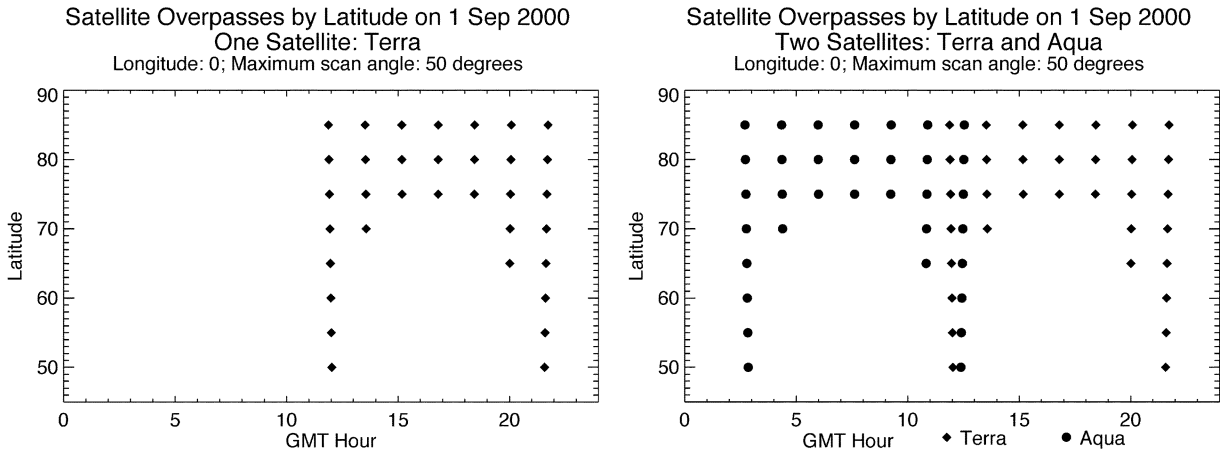

(a) (b)

Fig. 2. Time differences between successive overpasses of the Terra satellite (a) as a function of latitude over the course of a 24-hour period at the Prime Meridian, and (b) for both Terra and Aqua. Only overpasses with sensor view angles less than 50° are considered.

with rms differences less than 5 m/s. Turner and Warren [22] obtained useful cloud track wind information from AVHRR Global Area Coverage (GAC) data in the Weddell Sea, Antarctica. The manual intervention required in these case studies did not allow for routine production.

In this paper, we present a fully automated methodology for estimating tropospheric motion vectors (wind speed, direction, and height) using the Moderate-Resolution Imaging Spectroradiometer (MODIS) onboard the National Aeronautics and Space Administration's (NASA) polar orbiting Terra and Aqua satellites. Orbital issues and retrieval methodology are discussed, and case study results are presented. The case study dataset is used in numerical weather prediction (NWP) model impact studies, where the effect of the MODIS winds on forecasts is assessed.

II. Orbital Issues

The wind retrieval methodology builds on the cloud and water vapor feature tracking approach used with geostationary satellites. It is therefore necessary to track features over time in a sequence of images. Statistical analyses of visible, infrared, and water vapor wind datasets from geostationary satellites versus rawinsonde data have shown that the optimal processing intervals are 5 min for visible imagery of 1-km resolution, 10 min for infrared imagery of 4-km resolution, and 30 min for water vapor imagery of 8-km resolution [25]. How often can we obtain successive images for wind vectors from a polar-orbiting satellite?

Not surprisingly, the answer depends on the latitude and the number of satellites. Fig. 2(a) shows the frequency of time differences between successive overpasses at a given latitude-longitude point during one 24-hour period with a single satellite (Terra). The points show only those overpasses where the sensor (MODIS) would view the earth location at an angle of 50° or less. At larger scan angles the sensor would view the area near the pole on every overpass. At 60° latitude, there are two overpasses separated by about ten hours and 13 hours. No useful wind information can be obtained at this latitude with only one satellite. At 80° there are many views separated by orbital period of 100 min, but there is still a 13-hour gap each day. For other longitudesm, the gap will occur earlier or later in the 24-hour period, so that the entire polar area will be covered by multiple overpasses over the course of a day. Although the 100-min

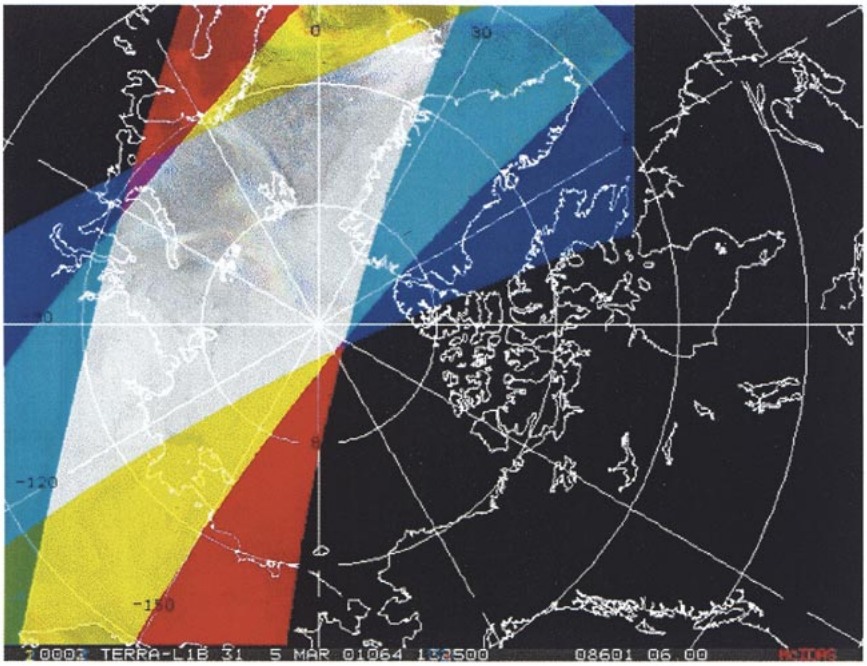

Fig. 3. Three successive MODIS orbits over the Arctic (red, green, blue). The overlap of the orbits (whitish-gray shade) is the area for which wind vectors can be estimated with each triplet of orbits.

temporal sampling is significantly longer than the optimal processing intervals for geostationary satellites, in theory wind vectors can be obtained during part of every day for the area poleward of approximately 70° latitude.

Fig. 2(b) shows the coverage with two satellites: Terra and Aqua. Temporal gaps of a few hours still exist at the lower latitudes of the polar regions, but at the higher latitudes the temporal coverage is very good. With additional satellites, e.g., the NOAA operational weather satellites with the AVHRR, it would be possible to obtain successive views of a given location within minutes of each other. Given that geostationary satellites provide reliable wind information equatorward of about 60° latitude, global coverage can be obtained if polar-orbiting satellites are used for high-latitude coverage poleward of 60°.

The methodology employed for wind vector estimation requires three successive images for wind retrievals. With geostationary satellites, the spatial coverage is constant. With a polar-orbiting satellite, the coverage from each successive orbit changes, so wind retrievals can only be done for the area of overlap between successive orbit triplets. This is illustrated for MODIS in Fig. 3. Three successive orbits are colored red, green, and blue; the overlap area is white-gray. For each 200-min time period (three successive orbits each separated by 100 min), wind vectors can be obtained for this area of overlap.

An additional orbital issue that must be considered is parallax, which is the apparent position displacement of cloud and water vapor features that results from nonnadir viewing angles. A cloud that is viewed off-nadir will appear to be further from the nadir position than it actually is. The greater the viewing angle, the greater is the displacement. For example, at 500 km from nadir the apparent location of a cloud with a height of 3 km will be approximately 2.1 km further from nadir than its actual position. At a distance of 1000 km from nadir the displacement is 4.5 km. The displacement is not the same from one orbit to the next, as the viewing geometry and the actual cloud position change. Appropriate corrections for this viewing geometry are needed, especially in the along-track corners of the overlapping region of the orbits where the errors in wind speed due to parallax are largest. Correction methods are under investigation.

Navigation accuracy plays only a minor role in wind retrieval. If the navigation error does not change within an image triplet, wind speed and direction errors will be minimal because they are calculated from relative positions. Navigation accuracy is important in the assignment of wind vector locations and, therefore, in the use of the wind vectors in numerical models. However, navigation errors for MODIS are very small relative to the size of model grid cells, so the impact is minimal.

III. Wind Retrieval Methods

Cloud and water vapor tracking with MODIS data is based on the established procedure used for GOES, which is essentially that described in [16], [17], [23], and [24]. With MODIS, cloud features are tracked in the infrared (IR) window band at 11 μm, and water vapor (WV) features are tracked in the 6.7-μm band.

After remapping the orbital data to a polar stereographic projection, potential tracking features are identified. The lowest (coldest) brightness temperature in the IR window band, generally indicating cloud, within a 13 $\times$ 13 pixel (26 $\times$ 26 km) target box is isolated, and local gradients are computed. Gradients that exceed a specified threshold are classified as targets for tracking. For water vapor target selection, local gradients are computed for the area surrounding every pixel rather than the single pixel with the minimum brightness temperature in a box. Water vapor targets are selected in both cloudy and cloud-free regions.

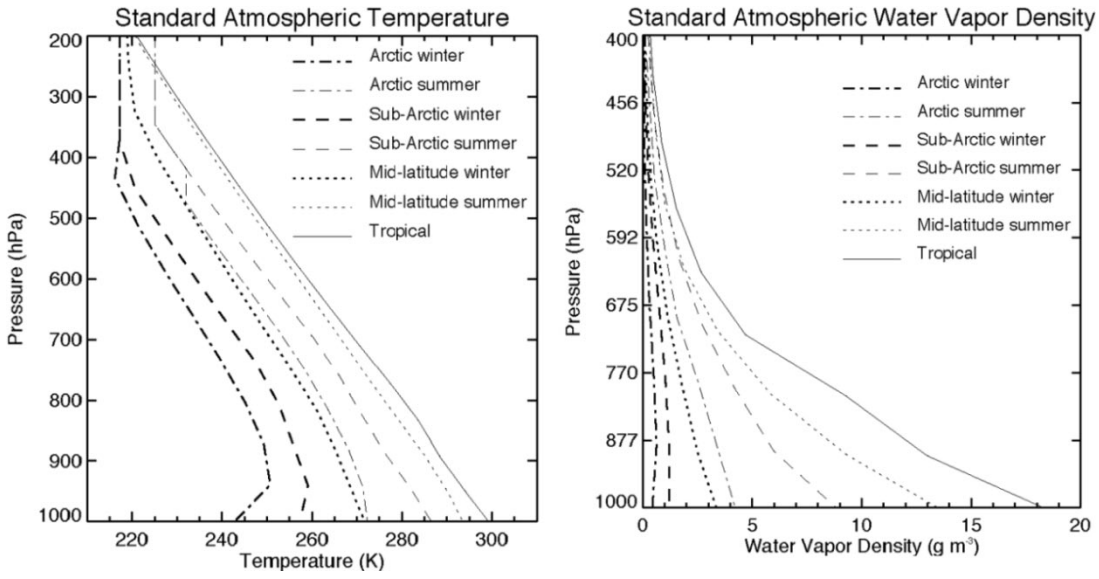

(a) (b)

Fig. 4. (a) Temperature and (b) humidity profiles for standard atmospheres and Arctic mean summer and winter.

The tracking method searches for the minimum of the sum of squared radiance differences between the target and the search boxes in two subsequent images. A model forecast of the wind is used to provide guidance on the appropriate search area for each target feature. Displacement vectors are derived for each of the two subsequent images. They are then subject to consistency checks to eliminate accelerations that exceed empirically determined tolerances and surface features that may have been misidentified as cloud.

Wind vector heights are assigned by any one of three methods. The infrared window method assumes that the mean of the lowest (coldest) brightness temperature values in the target sample is the temperature at the cloud top. This temperature is compared to a numerical forecast of the vertical temperature profile to determine the cloud height. The method is reasonably accurate for opaque clouds, but inaccurate for semitransparent clouds. The CO_2 slicing method works well for both opaque and semitransparent clouds. Cloudy and clear radiance differences in one or more carbon dioxide bands (e.g., 13.3, 13.6, 13.9, or 14.2 μm on MODIS) and infrared window bands are ratioed and compared to the theoretical ratio of the same quantities, calculated for a range of cloud pressures. The cloud pressure that gives the best match between the observed and theoretical ratios is chosen [15], [6]. The H_2O-intercept method of height determination can be used as an additional metric or in the absence of a CO_2 band. This method examines the linear relationship between clusters of clear and cloudy pixel values in water vapor-infrared window brightness temperature space, predicated on the fact that radiances from a single cloud deck for two spectral bands vary linearly with cloud fraction within a pixel. The line connecting the clusters is compared to theoretical calculations of the radiances for different cloud pressures. The intersection of the two gives the cloud height [19], [20]. The H_2O-intercept and CO_2 slicing methods do not work well with low-level or multilayered clouds.

The height of clear sky water vapor wind vectors is determined by comparing the water vapor brightness temperature to a collocated model temperature profile, analogous to the IR window method for cloud features. However, the brightness temperature of the feature being tracked corresponds more to a layer than a level, as will the retrieved wind vector height [18].

In the case study, the U.S. Navy Operational Global Atmospheric Prediction System (NOGAPS) model with 1.0° spatial resolution and 13 vertical levels was used. The number of vertical levels is a limitation of the current wind retrieval code, not the model data. The choice of the NWP forecast model might have some bearing on the height assignment accuracy. However, a comparison of two forecast models in geostationary wind retrieval shows that the bias and rms errors of the satellite winds when compared to radiosondes are nearly identical. For the polar winds differences might be larger, as the forecast models will be more dependent on model physics given the sparsity of data.

After wind vectors are determined and heights are assigned, the resulting dataset is subjected to a rigorous postprocessing, quality-control step. A three-dimensional (3-D) objective recursive filter is employed to reevaluate the tropospheric level that best represents the motion vector being traced, to edit out vectors that are in obvious error, and to provide end users with vector quality information [24].

IV. Atmospheric Considerations

Atmospheric and surface characteristics over polar regions require special consideration in the development of wind retrieval methods. The polar regions are characterized by low temperatures, ubiquitous atmospheric temperature inversions, low water vapor amounts, bright and cold surfaces, extensive cloudiness, and a high frequency of low, thin clouds. Low-level or surface-based temperature inversions are the rule rather than the exception. This is illustrated in Fig. 4, which gives standard temperature profiles based on data in [4], and Arctic mean profiles of temperature and humidity that are based on Arctic Ocean coastal and drifting station data described by Kahl *et al.* [10].

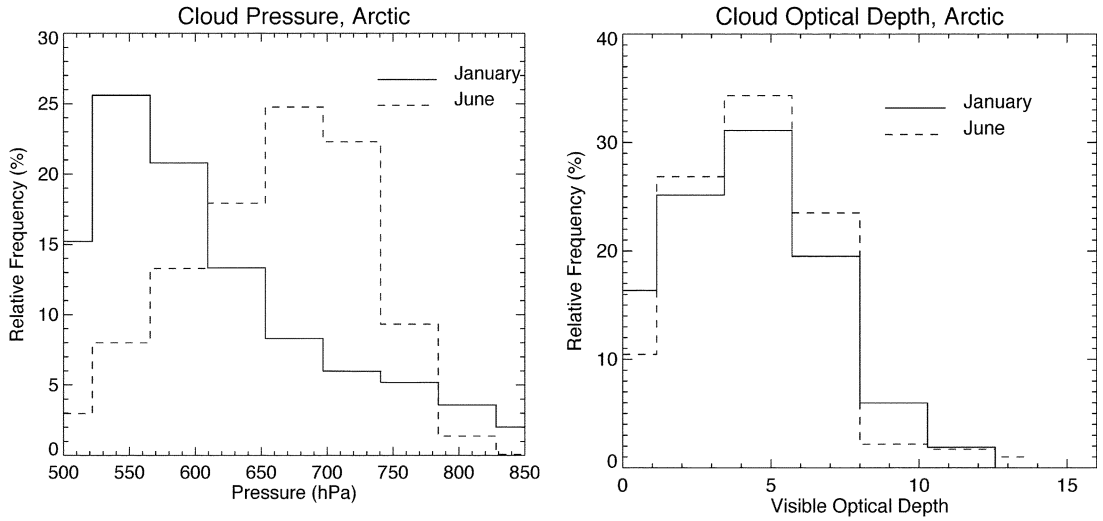

(a) (b)

Fig. 5. Relative frequency of (a) satellite-derived cloud top pressure and (b) visible optical depth for January and June in the Arctic. Data are from the extended AVHRR Polar Pathfinder project.

The Arctic and Antarctic atmospheres are very dry, with total precipitable water amounts of less than 1 cm in the winter and 1–2 cm in summer. Due to the low water vapor amounts, brightness temperature gradients in the 6.7-μm band are small, and surface emission can sometimes contaminate the radiances in clear sky areas. Nevertheless, as will be shown, the water vapor band has proven to be extremely useful in the estimation of polar winds. In fact, the lower water vapor amounts result in a greater number of wind retrievals lower in the atmosphere than is typically obtained in the midlatitudes and tropics.

Monthly average cloud amounts over the Arctic and Antarctica range from 50% to 90%, so cloud targets should be numerous. However, the predominant cloud type in the Arctic is marine stratus, with a spatial structure that generally produces fewer tracking features per unit area than other cloud types. A more significant problem occurs with vector height assignment for cloud-drift winds. The H_2O-intercept method is generally not useful for clouds lower in the atmosphere than about 600 hPa because upwelling radiation comes primarily from the atmosphere above the cloud, even in the relatively dry polar atmospheres. The CO_2 slicing method is very sensitive to the clear-cloudy radiance difference, and no height retrievals can be done if that difference is very small. The clear-cloudy radiance differences approach zero as the cloud temperature approaches the surface temperature, as is commonly the case for low clouds. In practice, the CO_2 slicing method is not useful for cloud pressures greater (cloud altitudes lower) than about 700 hPa.

Therefore, the infrared window method must be used for low cloud height assignment. With optically thick (opaque) clouds, the IR brightness temperature is a reasonable proxy for the cloud temperature. For thin clouds, the surface and atmosphere below the cloud may contribute significantly to the upwelling radiance. How common are low, thin clouds in the polar regions? Fig. 5 shows the relative frequency of cloud pressure and visible cloud optical depth over the Arctic in January and June from the AVHRR Polar Pathfinder (APP) project (cf., [13]). Clouds are thin during winter and summer, with the relative frequency of low clouds increasing during the summer. For the Antarctic (not shown) there is also a high frequency of low clouds (relative to the surface elevation). The implication of this for wind retrievals is that low cloud wind tracers need to be treated with caution.

V. Application

A 30-day case study is now described. The study period is March 5–April 3, 2001. MODIS Level 1B data from the Terra satellite were acquired from NASA's Goddard Distributed Active Archive Center (DAAC). The 1-km image data were normalized and destriped to reduce the effect of detector noise and variability. Two to four 5-min granules from each orbit were remapped into a polar stereographic projection at 2-km resolution and composited with the Man computer Interactive Data Access System (McIDAS; [11]). The resulting images are 2800×2800 pixels in size. Winds were derived from successive image triplets of the water vapor (band 27) and IR window (band 31) channels. Approximately 25 000 quality-controlled vectors, on average, were produced per day at each pole for the 30-day study period.

Figs. 6 and 7 give examples of the wind retrieval results for approximately half of the Arctic. Wind vectors are shown for half of the Arctic study area over a 12-hour period on the first day of the case study. Vectors at all vertical levels are shown, grouped into low (below 700 hPa), middle (400–700 hPa), and high (above 400 hPa) categories. Fig. 6 gives the results of IR cloud tracking, where vectors are plotted on the 11-μm image. There are approximately 4500 vectors in the image with most being in the low and middle height categories. Areas without wind retrievals are, for the most part, clear. Persistently cloudy areas such as the Norwegian Sea will typically have numerous cloud-drift wind vectors. Conversely, areas that are frequently clear, such as Greenland and eastern Antarctica, will have few cloud-drift wind vectors.

Fig. 7 gives the results of water vapor tracking, again for a 12-hour period on the first day. Vectors are plotted on the 6.7-μm water vapor image. There are about 13 000 vectors in the image, covering both clear and cloudy areas. In contrast to the cloud-drift wind vectors, the water vapor winds are primarily

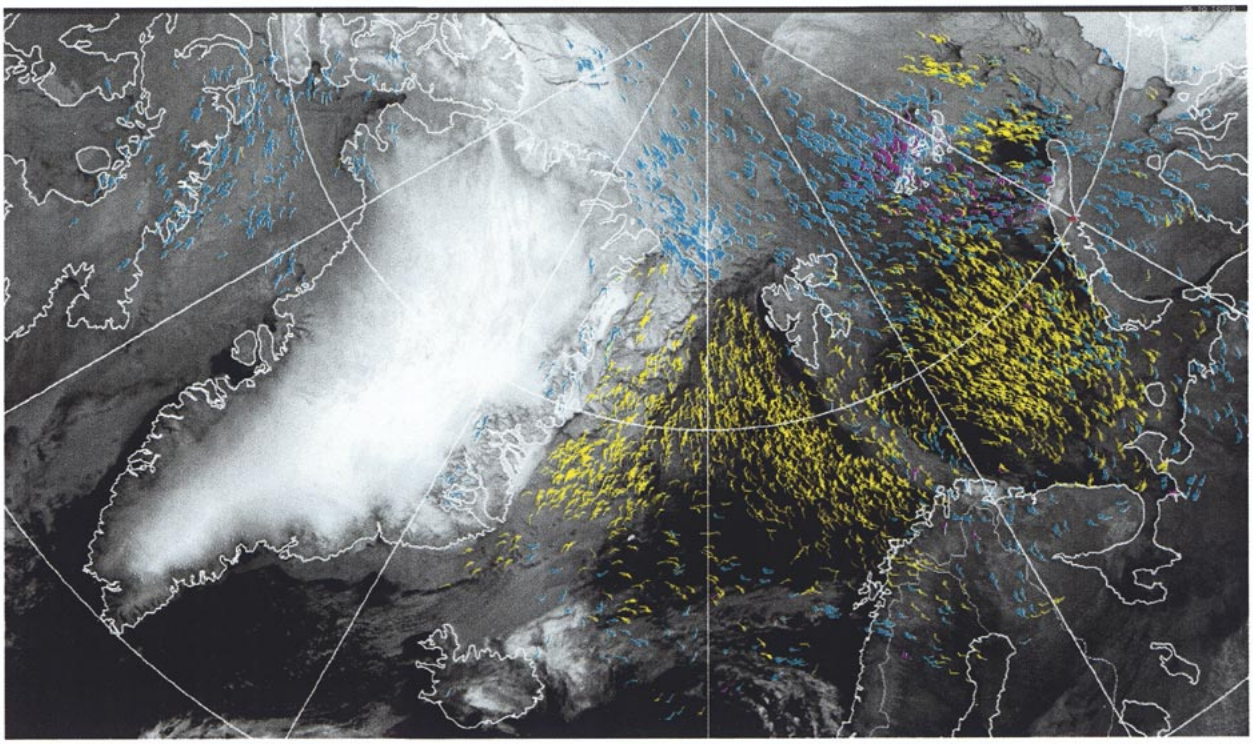

Fig. 6. Cloud-drift winds over the western Arctic from MODIS on March 5, 2001. The wind vectors are overlain on an 11-μm image covering Greenland and the Norwegian Sea. Vector colors indicate the height category: yellow is below 700 hPa; cyan is 700–400 hPa; magenta is above 400 hPa.

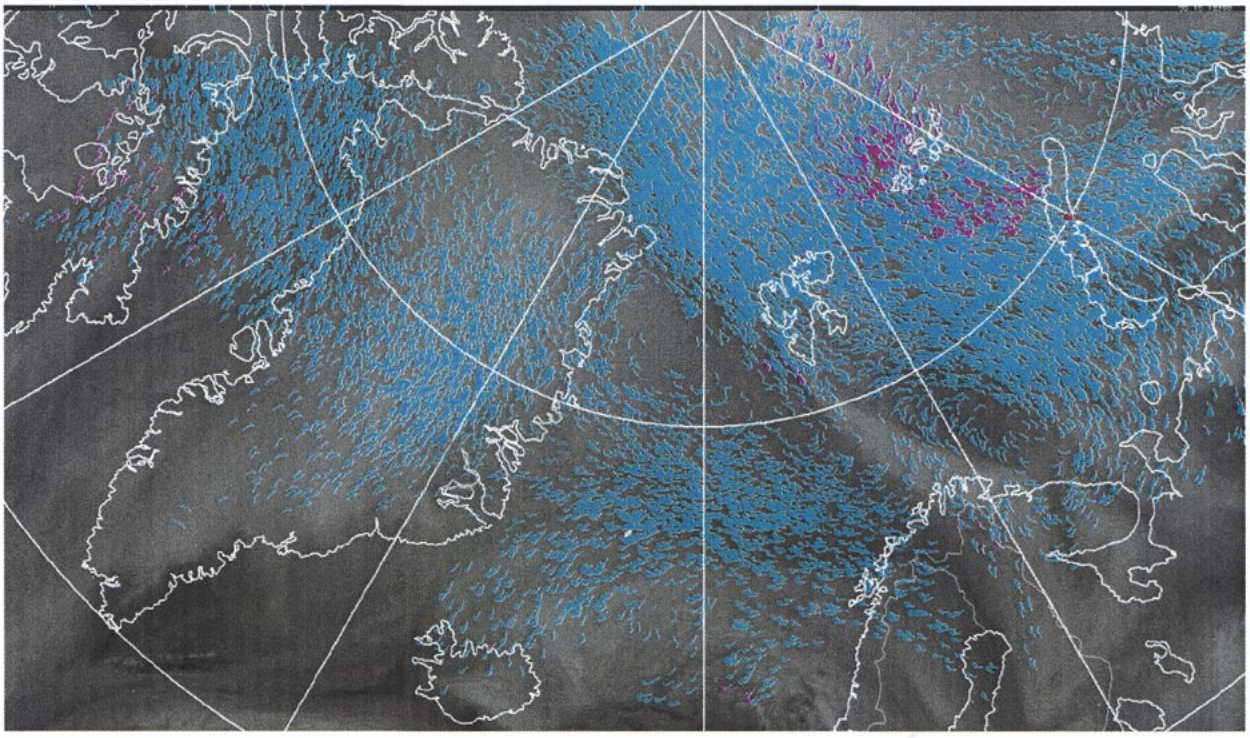

Fig. 7. Water vapor winds over the western Arctic from MODIS on March 5, 2001. The wind vectors are overlain on a 6.7-μm image covering Greenland and the Norwegian Sea. Vector colors indicate the height category: yellow is below 700 hPa; cyan is 700–400 hPa; magenta is above 400 hPa.

confined to the middle troposphere. The vast majority of the wind vectors from cloud-drift and water vapor tracking procedures come from the water vapor imagery. This fact certainly reduces the utility of imagers without water vapor channels, such as the AVHRR.

There are two common approaches to quantitatively assessing the quality of the wind vectors: comparing the satellite-derived winds with collocated rawinsonde observations, and evaluating their impact on numerical weather prediction. NWP studies are described in the next section. Statistics from comparisons with

rawinsondes can provide a measure of product quality over time and can aid in the determination of observation weights used in objective data assimilation. In the 30-day case study, the rms difference between the satellite winds and rawinsonde observations, averaged over all vertical levels, is 8.11 m/s with a speed bias of −0.58 m/s (satellite wind speed less than rawinsonde) for approximately 27 000 collocations with a mean wind speed of 14.9 m/s. All vectors within 1.5 hours and 200 km of the rawinsonde are used in the comparisons. The rms differences include errors in rawinsonde measurement and reporting, which are on the order of 3 m/s [9]. The rms and bias values are similar to, but slightly larger than, those for geostationary satellite winds. This is expected from the larger temporal sampling intervals. The best results are obtained for the middle and upper troposphere. Low-level rms differences are larger relative to the mean wind speed for reasons discussed earlier. As Fig. 1 illustrates, the verifying observational network is sparse so that these statistics do not necessarily apply uniformly to the entire Arctic and Antarctic.

VI. Impact of MODIS Winds on NWP Forecasts

While a polar winds product would be useful for a variety of meteorological and climatological applications, perhaps its most important contribution is in numerical weather prediction. Given the sparse rawinsonde observation network in the polar regions (Fig. 1) and the relative importance of high-latitude wind observations in model analyses noted by Francis [5], satellite-derived polar wind information has the potential to improve polar wind analyses and subsequently lead to improved forecasts. Model impact studies using the 30-day case study dataset were performed at ECMWF and the NASA Data Assimilation Office (DAO). The goal for both was to determine if forecasts are improved when MODIS winds are assimilated.

VII. ECMWF Impact Study

An initial model impact study was performed at the ECMWF with the 30-day case study dataset. All experiments employed a 3-D variational analysis assimilation scheme (3DVAR) with six hourly analyses that used the model first guess (FG) at the appropriate observation time [1], [3]. The model and analysis resolutions were T159 (approximately 125 km) with 60 levels in the vertical. Ten-day forecasts were run from each 12-UTC analysis.

Two experiments were conducted: the control experiment with routine observational data used as in operations, and the MODIS experiment with everything as in the control experiment plus the assimilation of MODIS winds. Over land, the IR and WV winds above 400 hPa were used. Over the ocean, IR winds above 700 hPa and WV winds above 550 hPa were used. These restrictions were chosen after trial experiments indicated a somewhat poorer quality of lower level winds, possibly due to height assignment problems over orography and ice and the use of relatively coarse resolution model data for the height assignment. As with operational wind vectors from geostationary satellite data, the MODIS winds were thinned to a 140-km resolution, and quality control in the assimilation was based on an asymmetric check against the first guess [21]. After thinning and quality control, the percentages of IR, cloudy WV, and clear WV winds used in the southern hemisphere are 10%, 5%, and 13%, respectively. For the northern hemisphere the corresponding values are 8%, 10%, and 13%.

TABLE I
First Guess Statistics for all IR MODIS Winds From the Control Experiment

	Southern Hemisphere	Northern Hemisphere
Low-level (below 700 hPa)		
NRMSVD	0.64	0.41
Speed bias (observation-FG) (m/s)	1.36	0.54
Mean model speed (m/s)	9.66	12.80
Number of cases	15,319	62,088
Mid-level (400-700 hPa)		
NRMSVD	0.49	0.38
Speed bias (observation-FG) (m/s)	0.56	0.30
Mean model speed (m/s)	14.43	14.70
Number of cases	90,462	78,892
High-level (above 400 hPa)		
NRMSVD	0.40	0.37
Speed bias (observation-FG) (m/s)	-1.38	0.31
Mean model speed (m/s)	21.47	19.49
Number of cases	19,037	3,490

Tables I and II give the first guess statistics from a passive comparison of the MODIS infrared and water vapor cloud winds, respectively, against the first guess used in the assimilation. The tables give the normalized rms vector difference (NRMSVD), the wind speed bias, the mean wind speed, and the number of cases that were used in the statistics. The NRMSVD is defined as the rms vector difference divided by the mean wind speed. As with the rawinsonde comparisons, for most levels and regions the NRMSVD and the speed bias are similar to or slightly poorer than other extratropical satellite-derived winds currently assimilated by ECMWF. This highlights the acceptable quality of the MODIS winds. The current exception is at lower levels in the Antarctic region where the monitoring statistics reveal large rms vector errors and relatively strong, fast speed biases (reaching 1.3 m/s). These poorer statistics motivated the cautious use of the MODIS winds at lower levels.

Globally, the fit of other observations against the first guess or the analysis is not significantly altered when MODIS winds are assimilated. This is also true locally for wind observations from rawinsondes, pilot reports, or aircraft observations for the Arctic region. This lack of change of the first guess fit to other observations suggests that the MODIS winds do not disagree with the rest of the observing network in the Arctic and is thus a

TABLE II
FIRST GUESS STATISTICS FOR ALL WV CLOUD MODIS WINDS FROM THE CONTROL EXPERIMENT

	Southern Hemisphere	Northern Hemisphere
Mid-level (400-700 hPa)		
NRMSVD	0.60	0.37
Speed bias (observation-FG) (m/s)	1.39	-0.36
Mean model speed (m/s)	12.55	15.06
Number of cases	282,527	207,324
High-level (above 400 hPa)		
NRMSVD	0.41	0.34
Speed bias (observation-FG) (m/s)	-0.51	0.70
Mean model speed (m/s)	21.29	20.86
Number of cases	80,083	23,196

positive aspect. Over the Antarctic region, a degradation of the first guess fit against rawinsondes suggests some disagreement between the MODIS winds and rawinsonde winds, at least over the coastal areas where most of the rawinsonde observations are made. This may indicate a poorer quality of the MODIS winds in these areas, or problems resulting from the coarse vertical and horizontal resolution of the forecast fields used in the height assignment for MODIS winds. Future experiments will employ the full resolution ECMWF fields in the data processing.

The mean polar wind analysis is considerably different in the experiment with MODIS winds. The differences for the Arctic are largest over the sea ice, with differences up to 3 m/s at all levels. The MODIS winds act to strengthen the circulation at upper levels, whereas at lower levels the difference field suggests a weakening of the local circulation. There are some indications that MODIS winds correct deficiencies in the Arctic flow field in the model in this case, e.g., the u-component bias between the Canadian Arctic profiler data and the first guess is slightly smaller, while the fit of other observations against the first guess is unaltered.

There is a significant positive impact on forecasts of the geopotential heights when MODIS winds are assimilated, particularly over the Northern Hemisphere. Fig. 8 shows the improvement in forecasts of the 1000 and 500 hPa geopotential heights over the Arctic (north of 65° latitude) when the MODIS winds are assimilated. The figure shows the correlation between the forecast geopotential height anomaly and the verifying analysis with the forecasts from the MODIS and the control experiments each validated against their own verifying analyses. The forecast improvements are significant at the 98% confidence level or better (t-test) at most vertical levels for a forecast range of two to five days.

The geopotential height forecast over Antarctica is also improved (not shown) by the inclusion of the MODIS winds, though the impact for the Southern Hemisphere is mainly neutral overall. There are a number of possible reasons for the less positive impact over the Southern Hemisphere. First, height assignment of the MODIS winds is more difficult over the high and steep orography of the Antarctic continent, in part because the spatial resolution of the models is low enough to smooth the steep orographic gradients. Second, fewer MODIS winds are used over Antarctica because winds below 400 hPa over land are not assimilated. Third, verification of forecasts in the Southern Hemisphere is hampered by fewer observations and thus smoother verifying analyses. The addition of MODIS winds is likely to increase the variability of these analyses over the Southern Hemisphere, making an interpretation of forecast scores more difficult. Fourth, the synoptic meteorology during our case study period over the Antarctic region was much less active compared to the Arctic, thereby creating less of an opportunity for forecast impact.

VIII. DAO IMPACT STUDY

The MODIS winds were also tested in the next-generation assimilation system of the NASA Data Assimilation Office. This is a global 3-D system based on the flux-form semi-Lagrangian general circulation model of Lin and Rood [12], coupled with the Physical-space Statistical Analysis System (PSAS; [2]). The PSAS algorithm solves the Kalman Filter analysis equation globally, in the same way that a 3-D variational algorithm does, but calculations are carried out in observation space rather than in spectral space. The model resolution is $1.0 \times 1.25°$ latitude/longitude with 55 vertical levels. Analysis increments are calculated at $2.0 \times 2.5°$ for 25 levels. The MODIS winds were thinned to a $0.5° \times 0.5°$ resolution; winds were not otherwise excluded from the experiments.

First, a control experiment was performed for the MODIS test period including all the standard observations available for operational NWP purposes, but excluding the MODIS winds. At each analysis time and observation location the observation-minus-six-hour forecast residuals (OMF) were calculated. Next, an assimilation that included the MODIS winds was performed and the OMF residual was again calculated. This residual is calculated before the analysis is performed, so it is essentially a diagnostic of the consistency between the analysis background (the six-hour forecast) and the observations. The OMF residual for the assimilation that includes the MODIS winds was significantly smaller than in the control assimilation, especially at 500 hPa. This demonstrates that the observations are consistent with the dynamics of the model, and that the MODIS winds contain information that can be ingested and retained by the assimilation system. As a result, the short-range forecast becomes more consistent with the observations at the new analysis time.

Five-day forecasts were then run from the $0Z$ analyses on every other day of both the MODIS assimilation and the control assimilation. This was done for water vapor winds, IR winds, and for all MODIS winds together. The combined IR and water vapor winds experiment is discussed here. In the ECMWF study, both sets of forecasts were compared to their own verifying analyses. In the DAO study, they are instead verified against operational ECMWF analyses.

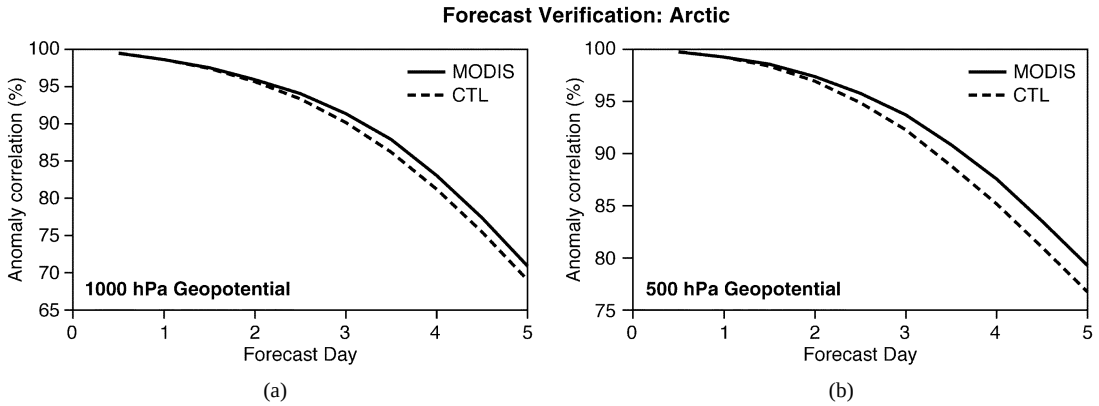

Fig. 8. Anomaly correlation as a function of forecast range for (a) the 1000-hPa and (b) the 500-hPa geopotential height forecast in the Arctic region for the ECMWF MODIS winds impact experiments. The MODIS experiment (solid) and the control experiment (dashed) have each been verified against their own analyses. The study period is March 5–29, 2001. The Arctic region is defined as the area north of 65° latitude.

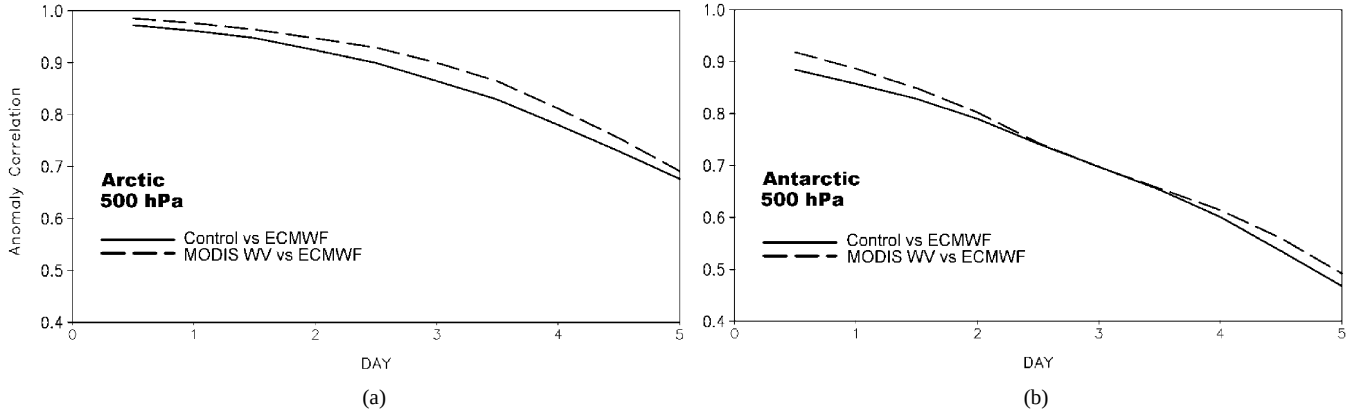

Fig. 9. Anomaly correlation as a function of forecast range for the 500 hPa geopotential height forecast over the Arctic (left) and Antarctic (right) from the DAO model impact study. The MODIS experiment (dashed) and the control experiment (solid) have each been verified against ECMWF analyses. The study period is March 5–29, 2001. The Arctic and Antarctic are defined as the area poleward of 60° latitude.

Fig. 9 shows the 500-hPa forecast score (anomaly correlation) as a function of forecast day for the Arctic and Antarctic, both defined as the area poleward of 60° latitude. Forecasts from the MODIS winds assimilation scored significantly higher than the control experiment in the Arctic, and marginally higher in the Antarctic. Due to the lack of observations over Antarctica, the Southern Hemisphere result may therefore be less meaningful than the Northern Hemisphere result. For the extratropics of each hemisphere (not shown), the MODIS winds improved the forecast skill in the Northern Hemisphere while the Southern Hemisphere impact was neutral to slightly positive. Again, errors in vector height assignment may explain the smaller impact in the Southern Hemisphere.

IX. Conclusion

This paper has demonstrated the feasibility of deriving tropospheric wind information at high latitudes from polar-orbiting satellites. The cloud and water vapor feature tracking methodology is based on the algorithms currently used with geostationary satellites, modified for use with the polar-orbiting MODIS instrument on the Terra and Aqua satellites. Orbital characteristics, low water vapor amounts, a relatively high frequency of thin, low clouds, and complex surface features create some unique challenges for the retrieval of high-latitude winds.

Nevertheless, model impact studies with the MODIS polar winds conducted at ECMWF and the NASA Data Assimilation Office are very encouraging. A 30-day case study dataset was produced and assimilated in the ECMWF and DAO models to assess forecast impact. When the MODIS winds are assimilated, forecasts of the geopotential height for the Arctic, Northern Hemisphere (extratropics), and the Antarctic are improved significantly in both impact studies. The forecast impact over the Southern Hemisphere extratropics is generally neutral.

The vast majority of the MODIS polar wind vectors come from tracking features in the water vapor imagery. This fact reduces the utility of imagers without water vapor channels for wind retrieval, such as the current operational AVHRR instrument. It also provides strong support for a water vapor channel on the Visible Infrared Imager/Radiometer Suite (VIIRS) that will be flown on the National Polar-Orbiting Operational Environmental Satellite System (NPOESS).

Improvements in height assignment, parallax corrections, and the use of additional spectral channels are under investigation. Progress in any of these areas can be expected to increase the impact of the MODIS polar winds on model forecasts. The impact of these wind datasets should be further enhanced with the use of 4D variational data assimilation techniques. Near real-time processing of MODIS data has just begun, providing a robust dataset for impact studies and meteorological applications. The

addition of Aqua MODIS data to Terra MODIS data will allow for even better coverage of the polar regions on a daily basis.

REFERENCES

[1] E. Andersson, J. Haseler, P. Unden, P. Courtier, G. Kelly, D. Vasiljevic, C. Brankovic, C. Cardinali, C. Gaffard, A. Hollingsworth, C. Jakob, P. Janssen, E. Klinker, A. Lanzinger, M. Miller, F. Rabier, A. Simmons, B. Strauss, J.-N. Thepaut, and P. Viterbo, "The ECMWF implementation of three-dimensional variational assimilation (3D-Var). Part III: Experimental results," *Q. J. R. Meteorol. Soc.*, vol. 124, pp. 1831–1860, 1998.

[2] S. E. Cohn, A. da Silva, J. Guo, M. Sienkiewicz, and D. Lamich, "Assessing the effects of data selection with the DAO physical-space statistical analysis system," *Mon. Weather Rev.*, vol. 126, pp. 2913–2926, 1998.

[3] P. Courtier, E. Andersson, W. Heckley, J. Pailleux, D. Vasiljevic, M. Hamrud, A. Hollingsworth, F. Rabier, and M. Fisher, "The ECMWF implementation of three-dimensional variational assimilation (3D-Var). Part I: Formulation," *Q. J. R. Meteorol. Soc.*, vol. 124, pp. 1783–1807, 1998.

[4] R. G. Ellingson, J. Ellis, and S. Fels, "The intercomparison of radiation codes used in climate models: Long wave results," *J. Geophys. Res.*, vol. 96, no. D5, pp. 8929–8953, 1991.

[5] J. A. Francis, "Validation of reanalysis upper-level winds in the Arctic with independent rawinsonde data," *Geophys. Res. Lett.*, vol. 29, no. 9, May 2002.

[6] R. Frey, B. A. Baum, W. P. Menzel, S. A. Ackerman, C. C. Moeller, and J. D. Spinhirne, "A comparison of cloud top heights computed from airborne LIDAR and MAS radiance data using CO_2-slicing," *J. Geophys. Res.*, vol. 104, no. D20, pp. 24 547–24 555, 1999.

[7] L. D. Herman, "High frequency satellite cloud motion at high latitudes," in *Proc. 8th Symp. Meteorological Observations and Instrumentation*, Anaheim, CA, Jan. 17–22, 1993, pp. 465–468.

[8] L. D. Herman and F. W. Nagle, "A comparison of POES satellite derived winds techniques in the Arctic at CIMSS," in *Proc. 7th Conf. Satellite Meteorology and Oceanography*, Monterey, CA, June 6–10, 1994, pp. 444–447.

[9] W. E. Hoehne, "Precision of National Weather Service upper air measurements," NOAA, Tech. Memo. NWST&ED-16, 1980.

[10] J. D. Kahl, M. C. Serreze, S. Shiotani, S. M. Skony, and R. C. Schnell, "*In situ* meteorological sounding archives for arctic studies," *Bull. Amer. Meteorol. Soc.*, vol. 73, no. 11, pp. 1824–1830, 1992.

[11] M. A. Lazzara, J. Benson, R. Fox, D. Laitsch, J. Rueden, D. Santek, D. Wade, T. Whittaker, and J. T. Young, "The Man computer Interactive Data Access System (McIDAS): 25 years of interactive processing," *Bull. Amer. Meteorol. Soc.*, vol. 80, no. 2, pp. 271–284, 1999.

[12] S.-J. Lin and R. B. Rood, "A flux-form semi-Lagrangian general circulation model with a Lagrangian control volume vertical coordinate," in *The Rossby-100 Symp.*, Stockholm, Sweden, 1998.

[13] J. Maslanik, J. Key, C. Fowler, T. Nyguyen, and X. Wang, "Spatial and temporal variability of surface and cloud properties from satellite data during FIRE-ACE," *J. Geophys. Res.*, vol. 106, no. D14, pp. 15 233–15 249, 2001.

[14] W. P. Menzel, "Cloud tracking with satellite imagery: From the pioneering work of Ted Fujita to the present," *Bull. Amer. Meteorol. Soc.*, vol. 82, no. 1, pp. 33–47, 2001.

[15] W. P. Menzel, W. L. Smith, and T. R. Stewart, "Improved cloud motion vector and altitude assignment using VAS," *J. Climate Appl. Meteorol.*, vol. 22, pp. 377–384, 1983.

[16] R. Merrill, "Advances in the automated production of wind estimates from geostationary satellite imaging," in *Proc. 4th Conf. Satellite Meteorology*. San Diego, CA: Amer. Meteorol. Soc., 1989, pp. 246–249.

[17] S. J. Nieman, W. P. Menzel, C. M. Hayden, D. Gray, S. T. Wanzong, C. S. Velden, and J. Daniels, "Fully automated cloud-drift winds in NESDIS operations," *Bull. Amer. Meteorol. Soc.*, vol. 78, no. 6, pp. 1121–1133, 1997.

[18] P. A. Rao, C. S. Velden, and S. A. Braun, "The vertical error characteristics of GOES-derived winds: Description and experiments with numerical weather prediction," *J. Appl. Meteorol.*, vol. 41, no. 3, pp. 253–271, 2002.

[19] J. Schmetz, K. Holmlund, J. Hoffman, B. Strauss, B. Mason, V. Gaertner, A. Koch, and L. van de Berg, "Operational cloud motion winds from METEOSAT infrared images," *J. Appl. Meteorol.*, vol. 32, pp. 1206–1225, 1993.

[20] G. Szejwach, "Determination of semi-transparent cirrus cloud temperatures from infrared radiances: Application to Meteosat," *J. Appl. Meteorol.*, vol. 21, p. 384, 1982.

[21] M. Rohn, G. Kelly, and R. W. Saunders, "Impact of a new cloud motion wind product from METEOSAT on NWP analyses," *Mon. Weather Rev.*, vol. 129, pp. 2392–2403, 2001.

[22] J. Turner and D. E. Warren, "Cloud track winds in the polar regions from sequences of AVHRR images," *Int. J. Remote Sens.*, vol. 10, no. 4, pp. 695–703, 1989.

[23] C. S. Velden, C. M. Hayden, S. J. Nieman, W. P. Menzel, S. Wanzong, and J. S. Goerss, "Upper-tropospheric winds derived from geostationary satellite water vapor observations," *Bull. Amer. Meteorol. Soc.*, vol. 78, no. 2, pp. 173–196, 1997.

[24] C. S. Velden, T. L. Olander, and S. Wanzong, "The impact of multispectral GOES-8 wind information on Atlantic tropical cyclone track forecasts in 1995. Part 1: Dataset methodology, description and case analysis," *Mon. Weather Rev.*, vol. 126, pp. 1202–1218, 1998.

[25] C. S. Velden, D. Stettner, and J. Daniels, "Wind vector fields derived from GOES rapid-scan imagery," in *Proc. 10th Conf. Satellite Meteorology*, Long Beach, CA, Jan. 9–14, 2000, pp. 20–23.

Jeffrey R. Key received the B.S. and M.S. degrees from Northern Michigan University, Marquette, in 1977 and 1982, respectively, both in environmental conservation, and the Ph.D. degree in climatology from the University of Colorado, Boulder, in 1988.

He joined the Advanced Satellite Products Team, National Oceanic and Atmospheric Administration, National Environmental Satellite, Data, and Information Service, Madison, WI, in 1999, where his goal is to improve high-latitude snow, ice, and atmospheric satellite products and foster their use in numerical weather prediction systems. His research interests include the radiative effect of clouds on the surface energy budget, polar meteorology, satellite remote sensing of cloud and surface properties, and climate change.

David Santek received the B.S. degree in atmospheric and oceanic science from the University of Michigan, Ann Arbor, in 1975, and the M.S. degree in meteorology from the University of Wisconsin, Madison, in 1978. He is currently pursuing the Ph.D. degree at the University of Wisconsin.

He has been with the University of Wisconsin's Space Science and Engineering Center for more than 20 years, working in the area of algorithm and software development for processing, analyzing, and visualizing data from space-based platforms. This has included data from the interplanetary Voyager spacecraft and the geostationary and polar-orbiting weather satellites.

Christopher S. Velden received the B.S. degree in natural science and geography from the University of Wisconsin, Stevens Point, in 1979, and the M.S. degree in meteorology from the University of Wisconsin, Madison, in 1982.

He is currently a Scientist at the Space Science and Engineering Center, University of Wisconsin and studies atmospheric tendencies and processes from the viewpoint of spaceborne instruments. He leads teams that are involved in developing techniques to track atmospheric motions from satellite imagery, as well as applications of satellite observations toward the monitoring of tropical cyclones and other weather phenomena.

Niels Bormann received the Dip. App. Sci. and Ph.D. degrees in geophysics/meteorology from Victoria University of Wellington, Wellington, New Zealand, in 1996 and 2000, respectively, having previously studied physics at Georg August Universität Göttingen, Göttingen, Germany. His Ph.D. research was concerned with the assimilation of humidity information from satellite data within a mesoscale model over New Zealand.

Since 2000, he has been working as a EUMETSAT Fellow at the European Centre for Medium-Range Weather Forecasts (ECMWF), Reading, U.K., investigating novel uses of satellite wind observations within ECMWF's global data assimilation system. His research interests include forecast impact studies regarding the assimilation of satellite data, characterization of observation errors and biases of satellite data, and general monitoring of remotely sensed data for use in numerical weather prediction.

Jean-Noël Thépaut received the title of "ingénieur de la météorologie" from Météo-France, Toulouse, France, in 1989, and the Ph.D. degree in meteorology from Université Paris VI, Paris, France, in 1992.

He is currently the Head of the Satellite Section of the Research Department, European Centre for Medium-Range Weather Forecasts (ECMWF), Reading, U.K. During and after his graduation, he participated to the development of the three- and four-dimensional variational data assimilation system at ECMWF and later at Météo-France, while working on the preparation for the assimilation from the European advanced sounder IASI. His research interests cover the general improvement of the use of satellite data in numerical weather prediction, in particular the assimilation of advanced infrared sounders and the assimilation of precipitation data.

Lars Peter Riishojgaard received the M.S. and Ph.D. degrees from the University of Copenhagen, Copenhagen, Denmark, in 1989 and 1992, respectively. both degree in geophysics.

Except for a year with EUMETSAT, Darmstadt, Germany (1999–2000), he has been with the Data Assimilation Office at the NASA Goddard Space Flight Center, Greenbelt, MD, since 1995, where he has studied the link between stratospheric dynamics and ozone variability, and he eventually designed and led the development of a three-dimensional ozone data assimilation system. In parallel with the ozone work, he carried out research in the area of state-dependent covariance modeling leading up to the design of a simplified implementation of a Kalman filter-like algorithm for a more general data assimilation system. Since August 2000, he has been leading the research and development work for the main DAO analysis system. His own research is now mainly focusing on the impact of existing and potential future satellite observations on assimilation and numerical weather prediction skill. He is also Deputy Director of the NASA/NOAA Joint Center for Satellite Data Assimilation.

Yanqiu Zhu received the B.S. degree in meteorology from Peking University, Beijing, China, in 1987, the M.S. degree in synoptic dynamics from the Chinese Academy of Meteorological Sciences, Beijing, China, in 1990, and the Ph.D. degree in geophysical fluid dynamics from Florida State University, Tallahassee, in 1998.

She is currently working at the Data Assimilation Office of NASA Goddard Space Flight Center, Greenbelt, MD, through the Science Applications International Corporation, Beltsville, MD. Her research interests have included parameter estimation, fixed-lag Kalman smoother-based retrospective data assimilation, and data impact studies.

W. Paul Menzel received the B.S. degree in physics from the University of Maryland, College Park, in 1967, and the M.S. and Ph.D. degrees in theoretical solid state physics from the University of Wisconsin, Madison, in 1968 and 1974, respectively.

In 1975, he joined the Space Science and Engineering Center, University of Wisconsin, where he was among the first to explore the possibilities for multispectral remote sensing of earth's atmosphere from a geosynchronous satellite. In 1983, he joined the National Oceanic and Atmospheric Administration, National Environmental Satellite, Data, and Information Service (NOAA/NESDIS), Madison, WI, to head the Advanced Satellite Products Team that developed, tested, and evaluated procedures for deriving new atmospheric products from spaceborne observations and transferred those from the research laboratory to the operational weather forecaster. He is currently Chief Scientist with the Office of Research and Application of NOAA/NESDIS, where he is responsible for conducting and stimulating research on environmental remote sensing systems, fostering expanded utilization of those systems locally and globally, and assisting in the evolution of the NOAA polar orbiting and geostationary satellite holdings.